Modeling the impact of hydrological changes on nitrate transport in the Mississippi River Basin from 1955 to 1994

Simon D. Donner, Michael T. Coe, John D. Lenters, Tracy E. Twine, and Jonathan A. Foley

Center for Sustainability and the Global Environment (SAGE), Institute for Environmental Studies, University of Wisconsin-Madison, Madison, Wisconsin, USA

Received 3 February 2001; revised 19 December 2001; accepted 19 December 2001; published 7 August 2002.

[1] The export of nitrate by the Mississippi River to the Gulf of Mexico has tripled since the 1950s primarily due to an increase in agricultural fertilizer application and hydrological changes. Here we have adapted two physically based models, the Integrated Biosphere Simulator (IBIS) terrestrial ecosystem model and the Hydrological Routing Algorithm (HYDRA) hydrological transport model, to simulate the nitrate export in the Mississippi River system and isolate the role of hydrological processes in the observed increase and interannual variability in nitrate export. Using an empirical nitrate input algorithm based on constant land cover and variability in runoff, the modeling system is able to represent much of the spatial and interannual variability in aquatic nitrate export. The results indicate that about a quarter of the sharp increase in nitrate export from 1966 to 1994 was due to an increase in runoff across the basin. This illustrates the pivotal role of hydrology and climate in the balance between storage of nitrate in the terrestrial system and leaching. *INDEX TERMS:* 4805 Oceanography: Biological and Chemical: Biogeochemical cycles (1615); 4845 Oceanography: Biological and Chemical: Nutrients and nutrient cycling; 1860 Hydrology: Runoff and streamflow; 1871 Hydrology: Surface water quality; *KEYWORDS:* nitrogen, Mississippi River, hydrology, nitrate flux, denitrification, aquatic biogeochemistry

1. Introduction

[2] Humans have more than doubled the rate of nitrogen (N) fixation in the biosphere, extracting roughly 100 Tg N per year from the atmosphere by the production of fertilizers, cultivation of nitrogen fixing crops, burning of fossil fuels, and other industrial activities [*Galloway et al.*, 1995]. The majority of this N is stored in soils and biota or returned to the atmosphere, but ~15% is exported to the world's rivers, primarily in the form of nitrate (NO_3^-), the most soluble and mobile form of N [*Caraco and Cole*, 1999].

[3] The leakage of NO_3^- from human activities, particularly agriculture, represents a serious threat to the freshwater, estuarine, and marine environment and represents a significant economic loss. Nitrogen is a limiting nutrient to primary productivity in estuaries and coastal waters worldwide. Anthropogenic NO_3^- has been linked to eutrophication and oxygen depletion in coastal waters, leading to the degradation of coastal ecosystems and fishing industries [*Diaz and Rosenberg*, 1995]. In addition, high NO_3^- levels and anoxic conditions promote denitrification, a source of nitrous oxide (N_2O), a powerful greenhouse gas and catalyst in the destruction of stratospheric ozone [*Naqvi et al.*, 2000; *Seitzinger and Kroeze*, 1998].

[4] The problem of NO_3^- export is particularly acute in the Mississippi River Basin, the world's third largest river basin and home to the majority of U.S. agricultural production (Figure 1). Nitrate export by the Mississippi River to the Gulf of Mexico tripled from the period 1955–1970 to the period 1980–1999, primarily due to a sixfold increase in N fertilizer application and an increase in runoff [*Goolsby et al.*, 2000]. This has led to an increase in the severity and extent of bottom water hypoxia in the northern Gulf of Mexico and contributed to increased benthic mortality and fisheries decline [*Rabalais et al.*, 1996; *Turner and Rabalais*, 1991; *Turner and Rabalais*, 1994]. U.S. federal and state negotiators have discussed a plan to reduce the Gulf of Mexico "dead zone," including a proposed 30% reduction in N export by the Mississippi [*Showstack*, 2000]. Integrated large-scale studies of the terrestrial and aquatic system will be vital to reaching these objectives.

[5] Understanding the causes of long-term trends and short-term variations in NO_3^- export poses a substantial scientific challenge. Nitrate export is extremely heterogeneous, dependent on a variety of factors including anthropogenic N inputs, hydrology, geology, and vegetation cover. Dynamic simulation of the variation in N loading and N export over time using solute transport models has only been conducted in small watersheds [e.g., *Ferrier et al.*, 1995; *Whitehead et al.*, 1997]. Studies of large river basins have estimated N loading by using empirical models [*Meybeck*, 1982; *Caraco and Cole*, 1999] or by integrating digital databases of N sources [*Goolsby et al.*, 1999; *Burkart and James*, 1999]. The relationship between N

0886-6236/02/2001GB001396$12.00

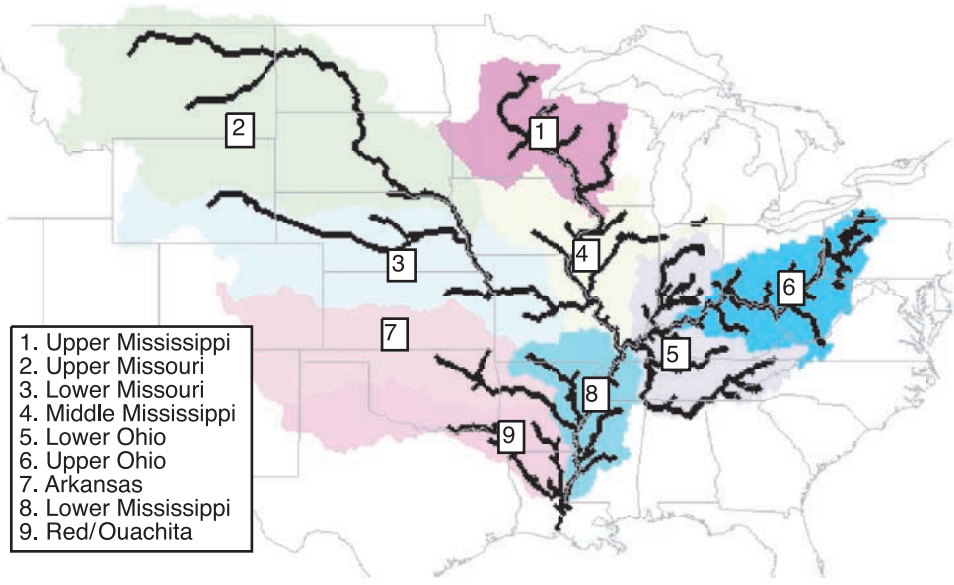

Figure 1. Map of Mississippi River Basin and large internal subbasins examined in this study. This map of the simulated Mississippi Basin was generated from topographic data and manually corrected river directions. Simulated area of each basin is within 10% of observations [*Goolsby et al.*, 1999]. Outlet of simulated Mississippi Basin lies just upstream of Old River Diversion, which maintains discharge of neighboring Atchafalaya River at ~30% of combined flow of Mississippi and Atchafalaya Rivers. Red/Ouachita Basin, which drains into Atchafalaya River, is therefore excluded from this study.

loading, observations of river discharge, and observations of N (or NO_3^-) export has then been described with regression analysis [*Caraco and Cole*, 1999; *Goolsby et al.*, 2000]. These regression models have been valuable in identifying the key variables that historically influenced NO_3^- export from large river basins like the Mississippi. But a physically based modeling system, similar to those used in small watersheds, is now needed to clearly assess the sensitivity of NO_3^- export to potential future changes in climate, land cover, and land management.

[6] This study is a first attempt to dynamically simulate NO_3^- export from a large river basin. We adapt two physically based models to simulate NO_3^- export in the Mississippi River system and assess the role of hydrological changes in the transport of NO_3^- to the Gulf of Mexico from 1955 to 1994. The development of this modeling system is a vital step toward research into the impact of changes in climate and land use on NO_3^- export.

2. Methodology

[7] We use the Integrated Biosphere Simulator (IBIS) land surface and terrestrial ecosystem model [*Foley et al.*, 1996; *Kucharik et al.*, 2000] and the Hydrological Routing Algorithm (HYDRA) hydrological transport model [*Coe*, 1998, 2000] to simulate the surface water budget of the Mississippi River Basin and transport of water and NO_3^- to the Gulf of Mexico. IBIS simulates surface and subsurface runoff from historical climate forcing for the period 1901–1994. HYDRA uses the runoff simulated by IBIS for 1955–1994 and uses NO_3^- leaching derived from a simple empirical algorithm to simulate both river discharge and NO_3^- export. By relying on the framework of an existing hydrology model, we can simulate the dynamic change in NO_3^- export over time in response to variability in hydrology and NO_3^- loading to the river system.

2.1. IBIS and HYDRA Model Description

[8] Both IBIS and HYDRA have been extensively tested and validated and are thoroughly documented elsewhere. Here we briefly describe the models and recent improvements.

[9] IBIS is a land surface and terrestrial ecosystem model that represents a wide range of phenomenon, including land surface biophysical processes (energy, water, and momentum exchange between soil, vegetation, and the atmosphere), canopy physiology (canopy photosynthesis and conductance), vegetation phenology (budburst and senescence), and long-term ecosystem dynamics (vegetation growth and carbon cycling). These processes are organized in a hierarchical framework and operate at different time steps, ranging from 60 min to 1 year. This allows for explicit coupling among ecological, biophysical, and physiological processes occurring on different timescales. IBIS uses climate forcing and basic physical principles to explicitly simulate the time-transient surface energy and water budget, including surface and subsurface runoff.

[10] HYDRA simulates the time-varying flow and storage of water in terrestrial hydrological systems, including rivers, wetlands, lakes, and human-made reservoirs [*Coe*, 1998, 2000]. The model derives river paths and potential lake and wetland volumes from digital elevation models of the land surface (Terrain Base, from the National Oceanic and Atmospheric Administration, National Geophysical Data

Center, Boulder, Colo.). The physical land surface of HYDRA is coupled to a linear reservoir model to simulate (1) the discharge of river systems, and (2) the spatial distribution (and volume) of large lakes and wetland complexes. River discharge and surface water volume are determined hourly from upstream inputs, local surface and subsurface runoff (from IBIS), precipitation (from climate data), evaporation from water surfaces (estimated by a simple energy balance model), and river velocity (based on topography).

[11] IBIS has been extensively tested and applied to biophysical and hydrological problems at large temporal and spatial scales [*Foley et al.*, 1996; *Costa and Foley*, 1997; *Kucharik et al.*, 2000; *Lenters et al.*, 2000]. HYDRA has been tested globally, against observed annual mean discharge and lake area [*Coe*, 1998], and has been used to investigate the accuracy of general circulation model simulations of equilibrium surface hydrology [*Coe*, 2000]. IBIS and HYDRA were recently linked and used to simulate the surface water balance of the continental United States for the period 1963-1995 [*Lenters et al.*, 2000] and to evaluate the impact of water resources management practices on water resources in northern Africa [*Coe and Foley*, 2001].

[12] This study extends previous work by *Lenters et al.* [2000] on the hydrology of the continental United States, including the Mississippi Basin, with IBIS and HYDRA. We expand that work by making numerous improvements to the models, including a new vegetation phenology routine in IBIS and the incorporation of new climate and soils inputs. A description of the phenology routine and the impact of model improvements on simulated hydrology is available at http://www.sage.wisc.edu.

2.2. Simulating Nitrate Export Within HYDRA

[13] Nitrate comprises the majority of the total N leached to rivers in the Mississippi and most large river basins [*Caraco and Cole*, 1999; *Goolsby et al.*, 2000]. Although some NO_3^- is removed during transport due to processes like denitrification, the majority of NO_3^- entering a river system reaches the ocean. We adapted HYDRA to simulate NO_3^- export including transport as a dissolved constituent in the river system and removal due to benthic denitrification.

2.2.1. Nitrate Transport

[14] To simulate the time-varying flux and aquatic storage of NO_3^- in the Mississippi River Basin, we added a solute transport function to the existing structure of HYDRA. Although this function is specifically tailored to NO_3^-, it can be adapted to study the transport of another semi-conservative dissolved chemical, regionally or globally.

[15] Nitrate transport and storage are simulated using a linear reservoir model, similar to that used for water in HYDRA [*Coe*, 1998]. The model determines the mass and concentration of NO_3^- in the river, lake, or wetland system, the removal due to in-stream processes and the flux of NO_3^- downstream. Storage and transport is described by the time-dependent change in three reservoirs (surface pool, subsurface pool, and river). The surface and subsurface leaching pools (N_s and N_d in kilograms) contain NO_3^- leaching from the terrestrial system to the river. The river reservoir (N_r in kilograms) contains the sum of locally derived NO_3^- and the upstream inputs. The change with time of the NO_3^- mass in the river reservoir is described by the differential equation

$$d(N_r)/dt = \sum N_{in} + (N_s/T_s + N_d/T_d)(1 - A_w) + P - \Delta C - L - (N_r/T_r),$$

where $\sum N_{in}$ is the sum of the fluxes of NO_3^- (in kg s^{-1}) from the upstream cells, A_w is the fractional water area in the grid cell, from 0 (no water) to 1 (lake or wetland covers entire cell), and T_s, T_d, and T_r are the residence times of the reservoirs (described in Appendix A). P is the flux of nitrate from points sources (industrial and municipal) directly into the river, ΔC is the rate of change in NO_3^- mass due to chemical transformations, and L is the rate of NO_3^- removal due to in-stream processes.

[16] Industrial and urban point sources (P) are not considered in this study since they constitute a small percentage of the total NO_3^- inputs to the Mississippi system [*Goolsby et al.*, 1999]. Additionally, the net change in NO_3^- mass due to transformations (ΔC) is assumed to be zero. The net input of NO_3^- from the primary transformation process, the nitrification of ammonium (NH_4^+) to nitrite (NO_2^-) and NO_3^-, is likely insignificant, since the mass of available NH_4^+ and NO_2^- rarely exceeds 5% of the mass of NO_3^- in Mississippi waters [*Goolsby et al.*, 1999; *Battaglin et al.*, 2001; *Peterson et al.*, 2001].

2.2.2. Nitrate Removal

[17] A variety of in-stream processes, including denitrification, biological uptake, fixation by cyanobacteria, and storage in sediments, can result in permanent removal of NO_3^- from the water column. Benthic denitrification, the reduction of NO_3^- to N_2 and N_20 gas by anaerobic bacteria in the sediment, is the primary removal process in well-oxygenated river systems like the Mississippi. It may be responsible for the removal of 0–75% of NO_3^- inputs to large river basins [*Howarth et al.*, 1996; *Seitzinger and Kroeze*, 1998; *Alexander et al.*, 2000].

[18] In this study, we assume that benthic denitrification is the only significant removal process; net biological uptake, sediment burial, and water column denitrification are all assumed to be zero. While biological assimilation and fixation can be significant in small, productive streams, high turbidity and low light attenuation limits productivity in large river systems like the Mississippi [*Alexander et al.*, 2000; *Goolsby et al.*, 2000; *Peterson et al.*, 2001]. In addition, much of the NO_3^- used for growth in rivers by phytoplankton is remineralized and eventually returned to the river as NO_3^- [*Seitzinger and Kroeze*, 1998; *Peterson et al.*, 2001]. Permanent sediment burial is only a significant loss of particulate N from the water column, not of dissolved forms of N like NO_3^- [*Howarth et al.*, 1996]. Lastly, rates of water column denitrification are extremely low, as it only occurs in cases of extreme oxygen depletion [*Seitzinger*, 1988].

[19] Previous empirical models and N budget studies have either assumed that denitrification is insignificant in large rivers or set denitrification losses to a fixed percentage of annual inputs [e.g., *Seitzinger and Kroeze*, 1998]. *Howarth*

et al. [1996] found that rates of NO_3^- loss due to benthic denitrification decrease with a ratio of mean river depth and residency time, reflecting the reduced contact time between river water and sediments (where denitrification occurs) in larger rivers. Subsequent N isotope analysis and N budgets of the Mississippi Basin concurred, suggesting that benthic denitrification is negligible in the deep main branch of the Mississippi and that the vast majority of NO_3^- loss occurs in interior watersheds and smaller tributaries [*Goolsby et al.*, 1999; *Alexander et al.*, 2000; *Battaglin et al.*, 2001].

[20] Simulating benthic denitrification in rivers is extremely difficult, given the lack of direct measurements. However, since denitrification is a bacterial process, rates of activity depend largely upon temperature, NO_3^- availability, and substrate area [*Seitzinger*, 1988; *Pattinson et al.*, 1998; *Garcia-Ruiz et al.*, 1998a, 1998b]. We have adapted a denitrification relationship developed by *Toms et al.* [1975] based on stream temperature, NO_3^- availability, and water renewal time, which has been applied to river systems in a variety of climates [*Whitehead et al.*, 1997; *Ferrier et al.*, 1995; P.G. Whitehead, personal communication, 1999]. The loss of NO_3^- due to benthic denitrification (L) is

$$L(\mathrm{kg\,s^{-1}}) = K_\mathrm{l} A_\mathrm{b} \times 10^{(0.0293T)} \mathrm{C_{NO3}},$$

where C_{NO3^-} is nitrate concentration (kg m^{-3}), A_b (m^2) is riverbed area, and T is the water temperature (°C), both described in Appendix C. This exponential temperature relationship, based on Michaelis-Menten kinetics, indicates a doubling in denitrification rate for approximately every 10°C increase in water temperature. K_l is the denitrification rate parameter (m d^{-1}), set to 0.04(min (Q_c/Q),1). Q is the simulated river discharge, and Q_c = 120 m^3 s^{-1} is the average discharge for a 2.5-m-deep river (determined from the depth-discharge rating curve used in the riverbed area calculation and described in Appendix B). The discharge-based adjustment to the rate parameter (min (Q_c/Q),1) reflects the reduction in sediment contact time with an increase in river depth (P.G. Whitehead, personal communication, 1999). This causes low denitrification rates in large, deep rivers [*Alexander et al.*, 2000]; in our study, it is only important in the main stem of the Mississippi and in the major tributaries.

[21] The mass of NO_3^- removed from the river system due to denitrification is determined at each time step. This enables analysis of the temporal and spatial variability in both denitrification rates (per unit time and area of riverbed) and rates of NO_3^- removal (percent of NO_3^- inputs removed due to denitrification).

2.3. Input Data

[22] IBIS was executed at a 0.5° × 0.5° latitude-longitude grid resolution over the Mississippi River Basin (29°N–50°N, 115°W–78°W), a 2.97 million km^2 region of the continental United States and southern Canada. The IBIS simulation was integrated from 1901 to 1994, following a 9-year climatological spin-up period. HYDRA simulations were conducted at a 5-min latitude-longitude grid resolution (~10 km) over the same region from 1955 to 1994, following a 5-year spin-up period used to generate background water and NO_3^- levels in the river system.

[23] The models required transient climate data and fixed inputs of soil texture, topography, and land cover type. The input data sources and NO_3^- leaching algorithm are described in sections 2.3.1–2.3.4.

2.3.1. Climate

[24] The climate input variables to IBIS include air temperature, precipitation rate, cloud fraction, relative humidity, wind speed, diurnal temperature range and number of wet days per month. In this study, monthly mean climate data for the period 1901–1994 was obtained from the Climatic Research Unit (CRU) of the University of East Anglia [*New et al.*, 2000]. Individual monthly mean data for wind speed, diurnal temperature range, and number of wet days per month was unavailable, so we used monthly climatological averages for the period 1961–1990. Daily and hourly variability for each variable was introduced using a statistical weather generator [*Richardson*, 1981; *Geng et al.*, 1985].

2.3.2. Soil Texture

[25] IBIS requires soil texture, in terms of fraction of sand, silt, and clay, for each of six soil layers down to 4 m. In this study, soil texture was derived from the Pennsylvania State University Earth System Science Center's CONUS data set [*Miller and White*, 1998]. The 30-arc-second resolution data set is based on the U.S. Department of Agriculture (USDA) State Soil Geographic Database, available at http://www.essc.psu.edu/soil_info/. The 11 soil layers in the CONUS data set were interpolated to the six IBIS layers using weighted averages. The lowest CONUS soil layer was missing a large percentage of data, so the top 10 CONUS layers were interpolated to the top five IBIS layers, and information from the fifth IBIS layer was duplicated in the sixth IBIS layer. The data was then aggregated to 0.5° resolution by performing a weighted average of the values.

2.3.3. Land Cover

[26] Vegetation type in IBIS was derived from the 1-km DISCover land cover data set [*Loveland and Belward*, 1997]. *Ramankutty and Foley* [1998] aggregated the original 94 land cover classes into 15 biomes and converted the data to 0.5° resolution by selecting the most dominant biome within each 0.5° grid cell.

[27] Both vegetation and cropland cover were used in the NO_3^- leaching algorithm employed by HYDRA. Cropland cover in the Mississippi Basin was derived from a 1992 North American data set [*Ramankutty and Foley*, 1999] that depicts the fraction of land covered by crops at a 5′ × 5′ (roughly 10 km) spatial resolution. The cropland area in each grid cell was further divided into individual crop classifications. For simplicity, we assumed that all croplands were corn, soybean, or wheat, which cover 90% of the croplands in the major agricultural regions of the Mississippi Basin. The percentages of crop area in each state covered by the three crop classes were determined from USDA planted area data for 1992 [*U.S. Department of Agriculture*, 1994]. The crop classification fractions were applied to each grid cell within the state, assuming that the distribution of crop type in the state's croplands is relatively homogeneous.

[28] The crop cover data was combined with the IBIS vegetation classifications to define the natural vegetation

Table 1. Nitrate Leaching Rates by Land Use Classification[a]

Land Cover Class	Nitrate Leaching Rate, kg ha^{-1}	Source
IBIS Biome		
Temperate needleleaf evergreen forest	0.32	(1)
Temperate deciduous forest	0.40	(1)
Boreal evergreen forest	0.14	(1)
Boreal deciduous forest	0.15	(1)
Evergreen/deciduous mixed forest	1.60	(1)
Savanna	0.40	(2), (3), (4)
Grassland/steppe	0.40	(2), (3), (4)
Dense shrubland	0.40	(2), (3), (4)
Open shrubland	0.40	(2), (3), (4)
Cropland		
Corn	8.50	(1)
Soybean	8.50	(1)
Wheat	0.80	(1)

[a] Shown are annual mean nitrate leaching rates employed by leaching algorithm. Rate represents amount of nitrate exported to aquatic system each year per area of land. Sources: (1) *Reckhow et al.* [1980], (2) *Loehr* [1974], (3) *Dodds et al.* [1996], (4) *Johnes* [1996].

type, the fractional vegetation coverage, and the fractional coverage of the three crop classes in each 5′ grid cell. We assume no significant change in crop cover since 1955; total crop cover in the United States has remained relatively constant since the 1950s, although soybean cultivation expanded into the Great Plains during the 1960s [*U.S. Department of Agriculture*, 1994; *Ramankutty and Foley*, 1999].

2.3.4. Nitrate Leaching Algorithm

[29] We developed a very simple NO_3^- leaching algorithm to roughly simulate the spatial and temporal variation in leaching throughout the Mississippi Basin. Nitrate leaching rates are determined each day from annual rates reported in the literature for different vegetation and crop types and from the daily variability in runoff. This simple empirical approach permits us to evaluate the ability of our model structure to simulate the impact of hydrologic variability on NO_3^- export. A physically based leaching model would be necessary to best evaluate the impact of land management (e.g., the increase in fertilizer application since the1950s) on NO_3^- export by the river system.

[30] Annual mean leaching rates for the nine natural vegetation classes and three crop classes in the Mississippi Basin were determined from reported estimates (Table 1). Reported rates for corn and soybeans are an order of magnitude larger than rates for wheat and natural vegetation, due to high rates of N fertilizer application in corn cultivation, N fixation by soybeans, and the common practice of rotating corn and soybean cultivation. The leaching rates were applied to the combined crop and vegetation cover data to determine annual mean NO_3^- leaching rates for the Mississippi Basin at the 5-min spatial resolution used by HYDRA (Figure 2).

[31] The algorithm was designed to roughly represent the spatial variation in annual mean NO_3^- leaching due to variations in crop and vegetation cover in the Mississippi Basin. The leaching rates implicitly include NO_3^- originating from agricultural activity, including fertilizer and fixation (by soybeans), and natural sources, including biological fixation, atmospheric deposition, and N mineralization. Together, these sources are likely responsible for >80% of the NO_3^- export by the Mississippi Basin [*Goolsby et al.*, 1999]. The export coefficients for croplands were derived from field studies conducted during the 1970s and therefore represent agricultural land management from the middle of our study period. Possible geographical variations in leaching rates within individual land cover classes due to variation in fertilizer application rates or agricultural practices across the Mississippi Basin were not considered. Municipal and industrial NO_3^- sources were also not explicitly considered. The leaching rates include atmospheric deposition of NO_3^-, but do not reflect observed variation in deposition across the Mississippi Basin.

[32] Daily variability in leaching rates was calculated in HYDRA using the annual mean rates and the IBIS simulated runoff. Previous research has indicated that NO_3^- accumuccumulated in the soil during dry periods is flushed to the river system during wet period. This was demonstrated by the massive increase in NO_3^- export during the 1993 Mississippi floods [*Creed and Band*, 1998; *Goolsby et al.*, 2000; *Carey et al.*, 2001]. A number of researchers have therefore noted a strong linear correlation between NO_3^- export from a watershed and runoff or streamflow [*Lucey and Goolsby*, 1993; *Creed and Band*, 1998]. To simulate the impact of hydrologic variability on NO_3^- leaching, the daily leaching rate (X_d, in kg s^{-1}) is determined from the annual mean (X_a, in kg s^{-1}) and the ratio of the daily runoff (R, in m s^{-1}) to the long-term average (R_{avg}),

$$X_d = X_a R / R_{avg}.$$

[33] Surface and subsurface NO_3^- leaching rates are determined from the IBIS simulated surface and subsurface. We assume that 80% of the NO_3^- enters through the subsurface. A series of sensitivity tests indicated that simulated nitrate export is not highly sensitive to the long-term average ratio of surface to subsurface nitrogen leaching.

[34] The algorithm therefore simulates the impact of local hydrologic variation on NO_3^- inputs to the river system, while maintaining the long-term mean leaching rates

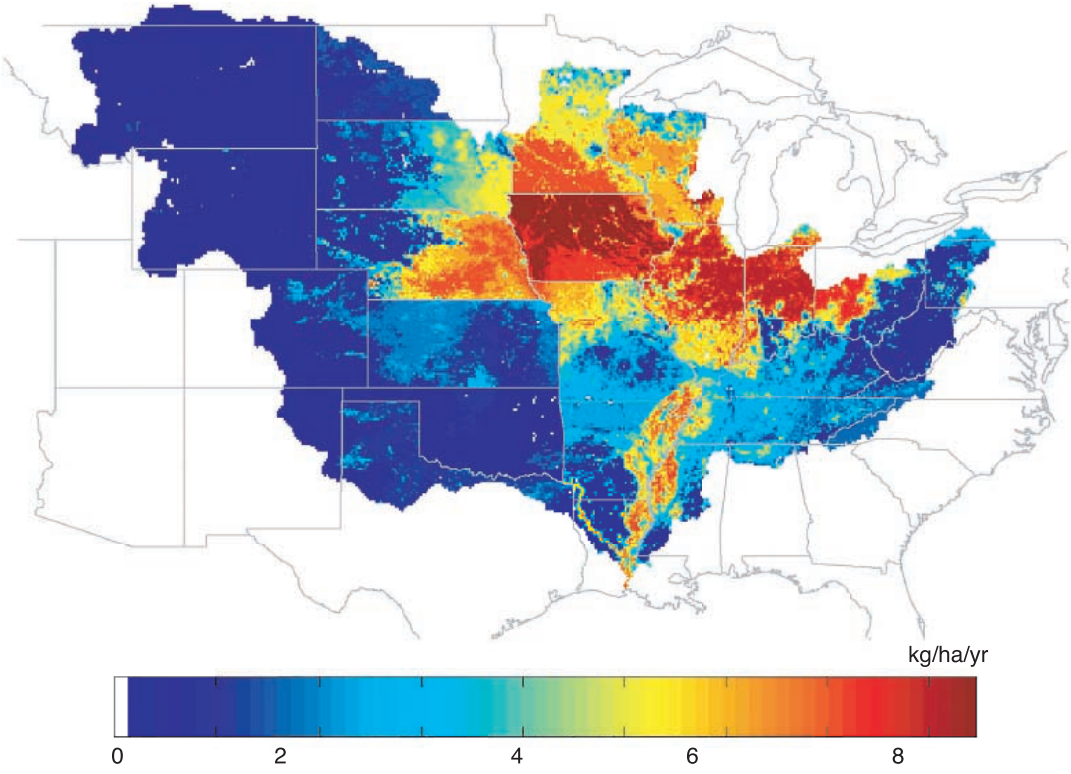

Figure 2. Annual mean nitrate leaching rate (kg ha^{-1} yr^{-1}) for 1955–1994 determined by nitrate leaching algorithm. Leaching rates are based on land cover classification and fractional crop area (corn, wheat, and soybean) at 5-min spatial resolution. Ratio of corn, soybean, and wheat planting per state was applied to the cropland area in each grid cell in the state. The sharp drop in estimated leaching rates at the Kansas border is due to the small area of corn and soybean planting in Kansas relative to neighboring states of Nebraska and Missouri.

indicated by the land cover characteristics. We intentionally ignored any changes in N inputs to the basin over the time period, like the observed increase in fertilizer application, to focus on the role of hydrology. By only considering the impact of temporal variability in hydrology on NO_3^- leaching, the algorithm is able to isolate the role of changes in terrestrial hydrology and, by association climate, in the increase in NO_3^- export from the Mississippi River since the 1950s.

3. Results

[35] We conduct this study in two steps. First, simulated river discharge in the Mississippi River Basin from 1965 to 1994 is evaluated against observed discharge. Second, simulated NO_3^- export within the Mississippi system is evaluated against U.S. Geological Survey (USGS) estimates. Separate simulations, with and without denitrification, are used to evaluate the denitrification function and to roughly quantify NO_3^- removal throughout the Mississippi Basin.

3.1. River Discharge

[36] We compare the simulated and observed river discharge at 29 stations throughout the Mississippi Basin from 1965 to 1994 to evaluate the ability of IBIS and HYDRA to simulate the hydrology of the basin (Table 2). The period of discharge analysis begins in 1965, rather than 1955, to coincide with available observations. The 29 stations selected are a subset of the nine large and 42 small internal subbasins examined in the analysis of NO_3^- export within the Mississippi Basin by *Goolsby et al.* [1999]. The other stations are excluded because of data limitations, overlapping basin area, or discrepancies in simulated basin shape. The Mississippi River at Vicksburg, Mississippi, is included because it is the station closest to the mouth with all 30 years of data.

[37] The drainage area and annual mean discharge for the 29 stations vary over 2 orders of magnitude. The observed daily discharge data were obtained from the USGS National Water Information Service (available from U.S. Geological Survey, National Water Information Service, at http://waterdata.usgs.gov/nwis/US) and converted to monthly and annual discharge for 27 of the stations. The observed monthly discharge data for Paducah, Kentucky, and Louisville, Nebraska, were obtained from the Global Monthly River Discharge Data Set (RivDIS) [*Vorosmarty et al.*, 1996]. Twenty-four of the 29 stations have data from 1965 to1994, with <2 years of data gaps; five stations (Paducah, Kentucky; Louisville, Nebraska; Metropolis, Ohio; Little Rock, Arkansas; and Desoto, Kansas) only have data from 1965 to 1984.

Table 2. Simulated and Observed Annual Mean River Discharge, 1965–1994[a]

River	Location	Basin Area, 10^3 km	River Discharge, $m^3 s^{-1}$		Error, %
			Observed	Simulated	
Cedar	Cedar Rapids, Iowa	12,260	145	144	−1
Scioto	Higby, Ohio	13,300	144	137	−5
St. Croix	St. Croix Falls, Wis.	16,200	142	92	−35
Grand	Sumner, Mo.	17,800	142	123	−13
Monogahela	Braddock, Pa.	19,000	356	293	−18
Muskingham	McConnellsville, Ohio	19,200	161	251	56
Chippewa	Durand, Wisc.	23,300	235	194	−17
Rock	Joslin, Ill.	24,700	209	144	−31
Tennessee	Whitesburg, Tenn.	25,610	1225	1228	0
Wisconsin	Muscoda, Wisc.	26,900	264	248	−6
Allegheny	Natrona, Pa.	29,800	580	450	−22
Mississippi	Royalton, Minn.	30,000	160	207	30
Iowa	Wapello, Iowa	32,400	282	215	−24
Osage	St. Thomas, Mo.	37600	334	309	−7
Minnesota	Jordan, Minn.	42,000	150	222	48
Illinois	Valley City, Ill.	68,800	312	405	30
Canadian	Calvin, Okla.	72,400	50	56	13
Wabash	New Harmony, Indiana	75,700	860	778	−10
Tennessee	Paducah, Ky.	104,500	1861	2742	47
Kansas	Desoto, Kans.	154800	239	26	9
Yellowstone	Sydney, Mont.	179,000	350	110	−69
Mississippi	Clinton, Iowa	221,700	1503	1449	−4
Platte	Louisville, Nebr.	222,200	201	360	79
Ohio River	Louisville, Ky.	236,130	3404	2943	−14
Missouri	Culbertson, Mont.	237,100	310	189	−39
Arkansas	Little Rock, Ark.	409,453	1082	1155	7
Ohio River	Metropolis, Ill.	525,700	8761	7557	−14
Missouri	Hermann, Mo.	1,357,700	2547	2460	−3
Mississippi	Vicksburg, Miss.	2,964,254	18320	17590	−4

[a] Shown are river name, station location, simulated basin area, observed and simulated annual mean discharge, and percent difference between simulated and observed discharge.

[38] Simulated annual mean discharge is within 20% of the observations for 16 of the 29 stations (Figure 3). There is a slight negative bias at Vicksburg (median −4.7%), closest to the mouth. Discharges from two of the major subbasins, the Upper Mississippi (Clinton, Iowa) and the Missouri (Hermann, Missouri), are within 4% of observations. The mean annual discharge from the Ohio River (Metropolis, Illinois), another major subbasin, is 13.7% below observations; this difference accounts for 72% of the difference of the error in mean annual discharge at Vicksburg.

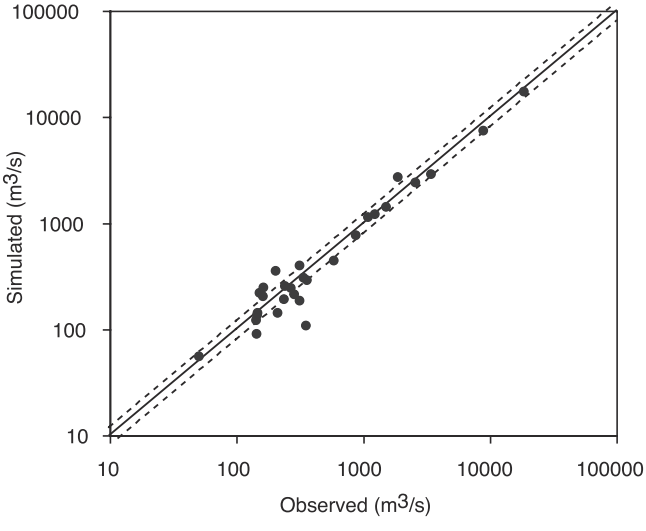

Figure 3. Plot of simulated versus observed annual mean river discharge ($m^3 s^{-1}$) from 1965 to 1994 for 29 stations in Mississippi Basin. Dashed lines represent values that differ by 20% from a 1:1 ratio between simulated and observed discharge.

[39] While there are large differences in simulated and observed annual mean discharge, the simulation of interannual variability in discharge is strong throughout the basin (Figure 4). The simulated and observed annual hydrograph of the Mississippi at Vicksburg (Figure 4a) and of the Tennessee River at Whitesburg (Figure 4c) demonstrate the model's ability to capture the annual variability in discharge. Even stations with substantial error in the magnitude of annual discharge, like St. Croix Falls (Figure 4b), exhibit strong agreement in interannual variability.

[40] There is an increasing trend in both observed (126 $m^3 s^{-1} yr^{-1}$) and simulated (118 $m^3 s^{-1} yr^{-1}$) discharge at Vicksburg (Figure 4a), which agrees with previous research on Mississippi discharge trends during the past century [*Baldwin and Lall*, 1999; *Goolsby et al.*, 1999]. Both the observed and simulated data suggest a 21% increase in discharge between the period 1955–1970 and the period 1980–1995, significant at the 99% level. This trend has been attributed to an increase in precipitation, particularly in the spring [*Baldwin and Lall*, 1999].

[41] The simulated long-term monthly discharge exhibits weaker agreement with observations than does simulated

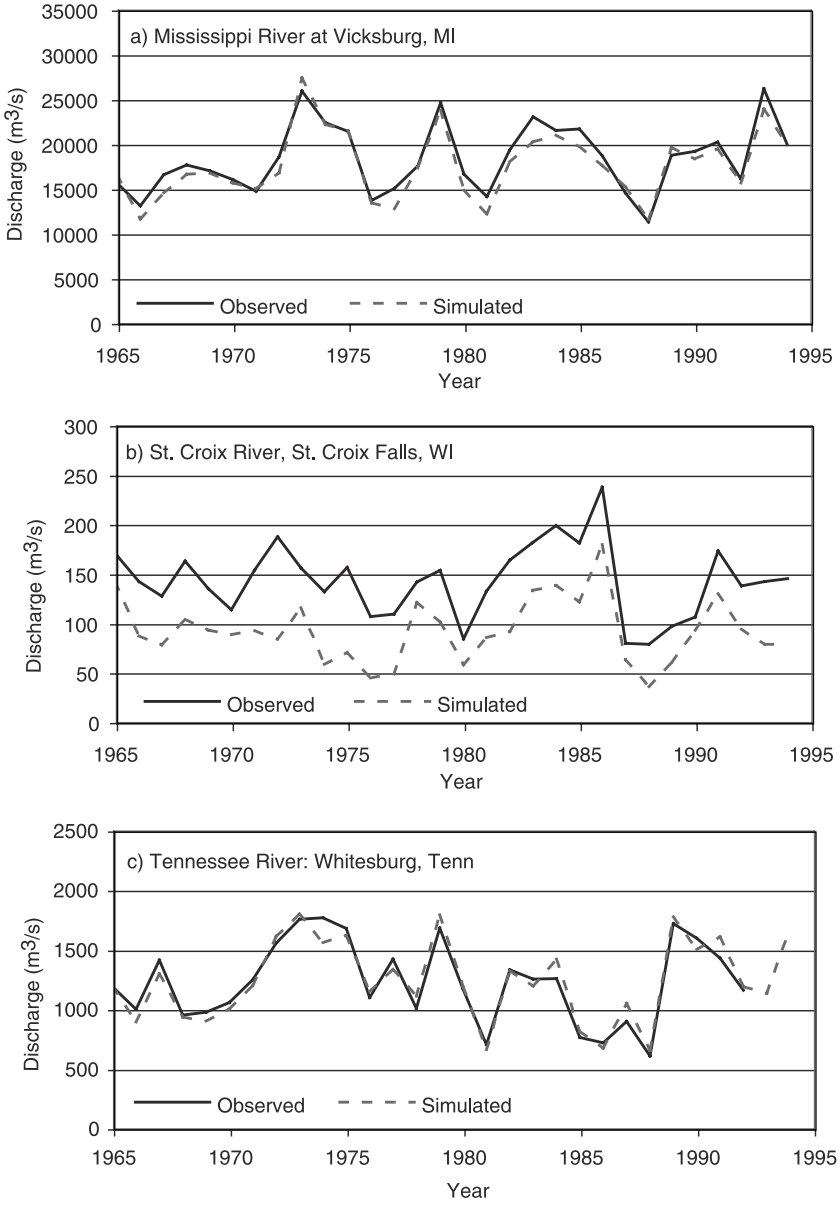

Figure 4. Simulated and observed annual discharge hydrograph ($m^3\ s^{-1}$) from 1965 to 1994 for (a) Mississippi River at Vicksburg, Mississippi, (b) St. Croix River at St. Croix Falls, Wisconsin, and (c) Tennessee River at Whitesburg, Tennessee.

annual discharge. The model underestimates the seasonality in discharge, particularly the magnitude of spring discharge, at several stations (Figure 5). The problem is most evident in the northern subbasins (e.g., St. Croix River), where IBIS poorly represents the peak in discharge due to spring snowmelt. Recent work on the water balance in IBIS suggests that this problem with seasonality is due largely to errors in the soil evaporation routine, estimates of soil depth, and the thermodynamic snow model. Efforts are currently underway to correct these errors in future versions of IBIS.

[42] The problems with the seasonal water balance, however, do not negate the ability of IBIS and HYDRA to simulate the annual water balance. The accuracy of simulations is summarized by histograms of the percent error in annual mean discharge, mean monthly discharge anomalies, and interannual anomalies for the 29 stations (Figure 6). All errors are calculated as a percentage of the annual mean discharge. The error in interannual anomalies (Figure 6c) is within 20% for the majority (76%) of the data, even though the error in seasonal anomalies (Figure 6b) is >20% for 65% of the station months.

[43] The error in timing and magnitude of the seasonal water cycle will affect the seasonality of NO_3^- leaching rates, which vary with simulated daily local runoff, and the seasonality of denitrification losses. But the successful simulation of interannual variability in river discharge

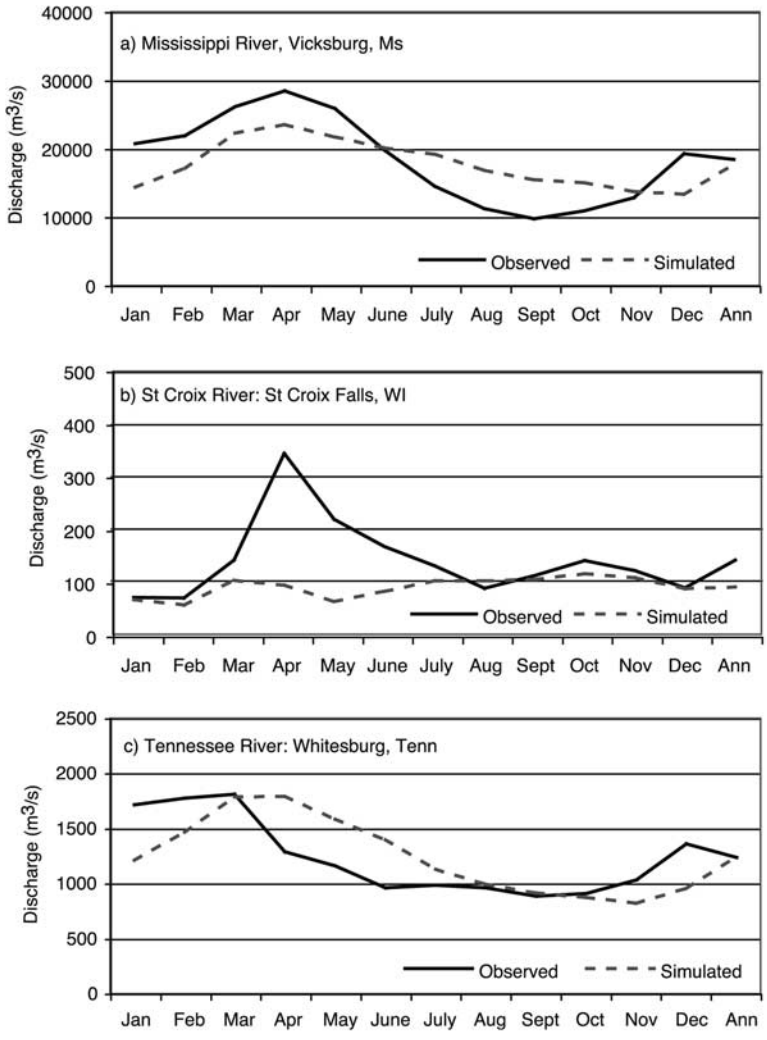

Figure 5. Simulated and observed mean monthly discharge ($m^3\ s^{-1}$) from 1965 to 1994 for (a) Mississippi River at Vicksburg, Mississippi, (b) St Croix River at St. Croix Falls, Wisconsin, and (c) Tennessee River at Whitesburg, Tennessee.

throughout the basin (<20% error) gives us confidence in the ability of IBIS and HYDRA to predict annual variability in terrestrial NO_3^- leaching and aquatic NO_3^- export.

3.2. Nitrate Transport

[44] After confirming the ability of IBIS and HYDRA to effectively simulate the hydrology of the Mississippi Basin, we used HYDRA and the NO_3^- leaching algorithm to simulate aquatic NO_3^- transport from 1955 to 1994. The objective is to evaluate whether HYDRA can simulate the variability in NO_3^- transport in a continental-scale river basin, even when forced with a simple leaching algorithm, and whether the model can isolate the role of hydrology in the observed increase in Mississippi NO_3^- export from 1955 to 1994.

[45] In section 3.2.1, we compare the simulated annual mean NO_3^- export to the *Goolsby et al.* [1999] estimates of NO_3^- export for a series of large and small Mississippi subbasins and examine the limitations of the leaching algorithm. In section 3.2.2, we analyze the role of hydrology in the increasing trend and interannual variability in NO_3^- export at St. Francisville, Louisiana (near the mouth), and at Clinton, Iowa (upstream of the Missouri and Ohio rivers). Last, in section 3.2.3, we analyze the role of benthic denitrification in the Mississippi Basin.

3.2.1. Mean Annual Nitrate Export in Mississippi River System

[46] The simulated annual mean NO_3^- export of the Mississippi River at St. Francisville from 1955 to 1994 is 635,719 t yr^{-1}, within 1% of the USGS estimate of 634,436 t yr^{-1} [*Goolsby et al.*, 2000]. Estimates of annual mean export since the 1950s are not currently available at other locations in the Mississippi Basin. However, *Goolsby et al.* [1999] determined the annual mean NO_3^- flux for the

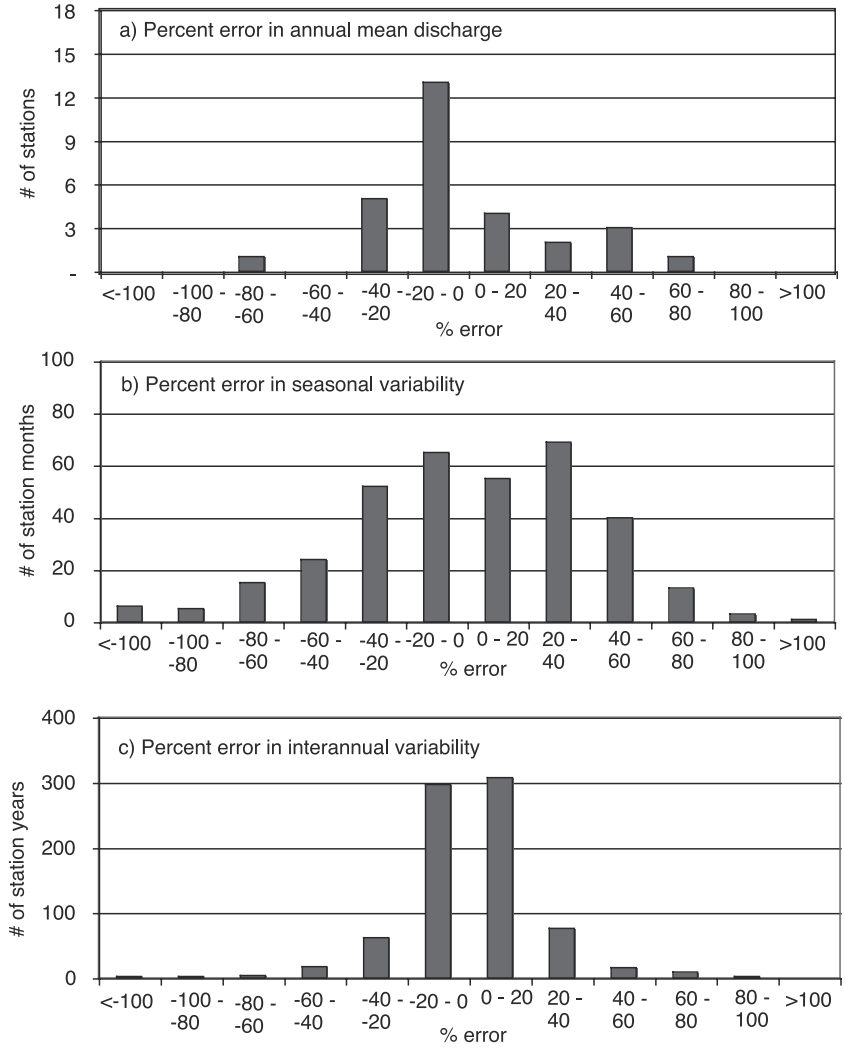

Figure 6. (a) Histogram of percent error in simulated annual mean river discharge from 1965 to 1994 (i.e., 100(sim-obs)/obs) for 29 stations listed in Table 2. (b) Histogram of percent error in simulated long-term seasonal cycle. Percent error is calculated as $100(sim_a\text{-}obs_a)/obs_a$, where sim_a and obs_a are deviations from mean monthly simulated and observed discharge and obs is observed mean annual discharge. Sample size is 384 (29 stations times 12 months, minus 36 months of missing data). (c) Similar to Figure 6b, but for interannual discharge anomalies from 1965 to 1994, excluding years with data gaps). Here sim_a and obs_a are annual rather than monthly anomalies, and sample size is 794 ($30 \times 29 = 870$, minus 76 years of missing data from 29 stations).

1980–1996 period at a series of river stations in the Mississippi Basin from point measurements of NO_3^- concentration and from a multiple regression model relating concentration to discharge and seasonality. We compare the simulated annual mean export and NO_3^- yield with USGS estimates for eight large and 24 small subbasins (Table 3). As in the river discharge analysis, several basins examined by the USGS are eliminated from this analysis, due to high standard error (>20%) in the USGS data, overlapping basin areas, or discrepancies in simulated river flow path or basin shape.

[47] The observed annual NO_3^- export from the Mississippi is significantly greater during the latter half of the 1955–1994 period due largely to an observed increase in N fertilizer application [*Goolsby et al.*, 1999]. In order to isolate the role of hydrology, we intentionally did not impose an increase in simulated NO_3^- leaching rates that would reflect the observed increase in N fertilizer application (discussed further in section 3.2.2). Therefore, the simulated export by the Mississippi is 23% lower than the USGS estimates for the period 1980–1996 (and, conversely, is 29% greater than USGS estimates for the period 1955–1979). As expected, the bias toward lower simulated NO_3^- export from 1980 to 1996 is greatest in the heavily fertilized central and eastern subbasins (e.g., Illinois and Iowa Rivers).

[48] Simulated NO_3^- export and yield is within 50% of USGS estimates for six of the eight large subbasins, but for only eight of the 24 small subbasins (Table 3). In general, simulated yield is too low in basins with high USGS

Table 3. Simulated and USGS Estimated Annual Mean Nitrate Flux, 1980–1994[a]

Large Basins	Location	Basin Area, 10 km^2	Nitrate Flux, t yr^{-1}		Error, %
			USGS	Simulated	
Mississippi	St. Francisville, La.	2,967,000	952,700	725,349	−24
Upper Mississippi	Clinton, Iowa	221,700	104,000	113,351	9
Missouri		1,357,700	125,900	222,985	77
Upper Missouri	Omaha, Nebr.	836,100	30,600	89,543	193
Lower Missouri	Hermann, Mo.	521,600	95,200	133,442	40
Ohio River		526,000	323,500	143,711	−56
Upper Ohio	Greensboro, Ohio	251,200	150,700	49,084	−67
Lower Ohio	Metropolis, Ill.	274,800	172,700	94,627	−45
Middle Mississippi		267,800	307,100	164,768	−46
Arkansas	Little Rock, Ark.	410,000	18,800	23,677	26
Lower Mississippi	St. Francisville, La.	184,000	54,200	56,857	5
Wabash	New Harmony, Indiana	75,700	97,100	46,588	−52
Wisconsin	Muscoda, Wis.	26,900	5660	11,701	107
Missouri	Culbertson, Mont.	237,100	560	6337	1032
Tennessee	Paducah, Ky.	104,500	24,010	28,232	18
Mississippi	Royalton, Minn.	30,000	880	11,879	1250
Minnesota	Jordan, Minn.	42,000	50,270	38,375	−24
Illinois	Valley City, Ill.	68,800	113,660	43,365	−62
Canadian	Calvin, Okla.	72,400	1010	2083	106
Platte	Louisville, Nebr.	222,200	12,380	35,557	187
Rock	Joslin, Ill.	24,700	30,800	14,641	−52
Cedar	Cedar Rapids, Iowa	12,260	33,280	17,740	−47
Iowa	Wapello, Iowa	32,400	57,450	27,569	−52
Des Moines	St. Francisville, Mo.	37,040	61,560	40,901	−34
Yellowstone	Sydney, Mont.	179,000	2780	3873	39
Kansas	Desoto, Kans.	154,800	7240	32,256	346
Grand	Sumner, Mo.	17,800	9480	16,222	71
Osage	St. Thomas, Mo.	37,600	5890	10,092	71
Arkansas	Tulsa, Okla.	193,300	9450	12,185	28
St. Croix	St. Croix Falls, Wis.	16,200	920	5109	455
Chippewa	Durand, Wis.	23,300	3920	9505	142
Allegheny	New Kensington, Pa.	29,800	13,610	4812	−65
Monogahela	Braddock, Pa.	19,000	11,100	1832	−83
Muskingham	McConnellsville, Ohio	19,200	14,590	3930	−73
Scioto	Higby, Ohio	13,300	18,230	8917	−51

[a] Shown are basin name, station location, catchment area, U.S. Geological Survey (USGS) estimated annual mean nitrate export (1980–1996), simulated annual mean nitrate export (1980–1994), and percent difference in simulated and USGS estimated export. Upstream contributions of nitrate are excluded (e.g., export for Lower Missouri equals flux from Missouri River at Hermann, Missouri, minus flux from Missouri at Omaha, Nebraska).

estimated NO_3^- yields and is too high in basins with low USGS estimated yields (Figure 7). An underestimate of the spatial heterogeneity in NO_3^- export is to be expected, since the annual mean NO_3^- inputs are based on broad land cover classifications. This approach is reasonably effective, however, at estimating NO_3^- export from large basins, as evidenced by the significant decrease in error with basin size (Table 3). It should be noted that the percent error is inflated by the extremely low USGS estimates of NO_3^- export; although simulated export from the Missouri at Culbertson, Montana, is 11 times greater than the USGS estimate, it amounts to only 5777 t NO_3^- yr^{-1}, <5% of the USGS estimated export from the Missouri Basin.

[49] The most significant error is the imbalance in simulated export for the Ohio and Missouri Basins. The USGS estimates that 34% of the total Mississippi NO_3^- originates in the Ohio Basin, versus 19% from HYDRA; the difference is reversed for the Missouri Basin, with 13% according to the USGS and 31% according to HYDRA (Table 4). The imbalance is largely due to the underestimate of NO_3^- leaching from heavily cultivated areas in the Lower Ohio Basin. An underestimate of export from more forested parts of the Upper Ohio Basin (e.g., Allegheny and Monogahela Basins) and an overestimate of export from the dry western portion of the Missouri Basin also play a role. A series of sensitivity tests, varying the export rates from wheat, corn, soybean, and natural vegetation individually and together by 25–100%, found that the relative contribution of the Ohio and Missouri Basins varied by <3%. The lack of sensitivity to changes in the input parameters in this region indicates some fundamental limitations of a simple land cover based leaching algorithm. Rather than increase the complexity of the algorithm to improve model fit, we examine the primary sources of error in the Ohio and Missouri Basin in order to identify the necessary variables in a future physically based N leaching model.

3.2.1.1. Inclusion of Other Crop Types

[50] The leaching algorithm divides all cropland area into corn, soybean, and wheat, assuming that other crop types represent a very small fraction of cropland area. In states like Nebraska and South Dakota, where other less N-intensive crops such as barley, alfalfa, sunflower, and oats are also produced in significant quantities, the assumption results in an overestimate of leaching rates. If these other crops have a mean NO_3^- leaching rate of only 1 kg ha^{-1} yr^{-1}, the simulated annual mean export from the Missouri River

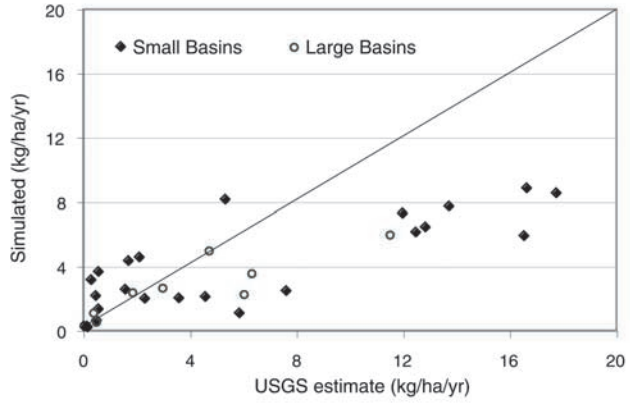

Figure 7. Scatterplot of simulated versus USGS estimated annual mean nitrate yield (kg ha^{-1} yr^{-1}) for eight large and 24 small Mississippi subbasins. Simulated yields are averaged over 1980–1994; USGS estimated yields are from period 1980–1996.

decreases by 20%, one third of the difference between the simulated and the USGS estimated export.

3.2.1.2. Heterogeneity in Soils and Climate

[51] Local soil properties (e.g., texture) and climate (e.g., precipitation), not reflected in the simple leaching algorithm, can affect both N mineralization and the soil N retention capacity, directly impacting the rate of NO_3^- leaching. High levels of soil organic carbon cause higher N mineralization rates in much of the Ohio and Upper Mississippi Basins than in the Missouri Basin [*Burkart and James*, 1999]. In addition, higher precipitation rates in the Ohio Basin should also result in greater rates of NO_3^- leaching from croplands.

3.2.1.3. Spatial Variation in Fertilizer Application Rates

[52] The variation in N fertilizer application rates across the Mississippi Basin [*Alexander and Smith*, 1990; *Wu and Babcock*, 1999], and thus NO_3^- leaching potential, is also not reflected in the simple land cover based leaching algorithm. The greater rates of N fertilizer application in states of the Ohio Basin reported by *Wu and Babcock* [1999] could account for 13–17% of the underestimate in export from the Ohio Basin, assuming the impact of greater N fertilizer application on leaching rates is relatively uniform in each state.

3.2.1.4. Altered Agricultural Drainage

[53] Artificially constructed streams, ditches, and underground tile drains, used to control runoff and sediment losses, increase the leaching of soluble agricultural chemicals like NO_3^- [*Randall et al.*, 1997]. According to a 1985 USDA survey, a larger percentage of cropland is artificially drained in Ohio (50%), Indiana (35%), and Illinois (35%) than in Missouri (25%), North Dakota (5%), and South Dakota (1%). Although the exact impact on NO_3^- export is difficult to quantify, the greater proportion of drained land suggests higher leaching rates in the Ohio Basin. Field research suggests artificial drainage could cause up to a 40% increase in simulated annual NO_3^- leaching [*Zucker and Brown*, 1998]. Excluding the effects of artificial drainage could therefore explain up to one third of the error in NO_3^- export from the Ohio River.

3.2.1.5. Other N Sources

[54] Since the leaching algorithm is based on broad land cover classes, it does not reflect the observed spatial variation in atmospheric N deposition or point source N inputs. The highest rates of dry and wet atmospheric N deposition occur in the Upper Ohio Basin, due to prevailing westerly winds and a higher concentration of power plants, industrial facilities, and people [*Goolsby et al.*, 1999; *Lawrence et al.*, 2000]. The observed variation in N deposition could explain over a third of the difference between simulated and USGS estimated NO_3^- export from the Upper Ohio River (assuming that a quarter is leached as NO_3^-). Point source N loading is also significantly greater in the Ohio Basin [*Goolsby et al.*, 1999]. Although point source N represents a tiny fraction of total N inputs, it enters directly into the river system, unlike other N sources. If one third of the point source N is exported as NO_3^- (point sources are often dominated by NH_4^+), it could account for an additional 15% of the error in NO_3^- export from the Ohio River.

[55] In general, the model underestimates the spatial heterogeneity in annual mean NO_3^- export, since the simple leaching algorithm does not reflect the regional variations in N inputs or NO_3^- processing capacity of the soil system. The problem is exacerbated in regions dominated by a particular land use or N source, like the heavily cultivated watersheds in the Lower Ohio Basin, the watersheds of the Upper Ohio Basin heavily impacted by atmospheric deposition, and the less productive rangelands of the Upper Missouri Basin. However, the coarse model is still able to capture the NO_3^- export from a large basin with a broader range of land cover types. For example, simulated annual mean export from the Upper Mississippi Basin, which contains a mixture of cropland, forest, and grassland, is within 7% of the USGS estimate. In addition, the simulated export from the entire Mississippi Basin, which integrates the Missouri River and the Ohio River, closely agrees with the USGS estimate. This gives us confidence in the ability of the model to simulate NO_3^- export from large basins.

3.2.2. Trend and Variation in Nitrate Export

[56] *Goolsby et al.* [1999] noted that NO_3^- export by the Mississippi River at St. Francisville, Louisiana, increased

Table 4. Subbasin Contribution to Total Nitrate Export, 1980–1994[a]

River Basin	USGS Estimated, %	Simulated, %
Upper Mississippi	10.9	15.6
Missouri	13.2	30.7
Upper Missouri	3.2	12.3
Lower Missouri	10.0	18.4
Ohio River	343.0	19.8
Upper Ohio	15.8	6.8
Lower Ohio	18.1	13.0
Middle Mississippi	32.2	22.7
Arkansas	2.0	3.3
Lower Mississippi	5.7	7.8

[a] Shown is percent of annual mean nitrate export by Mississippi River at St Francisville, Louisiana, originating in each subbasin. USGS estimated contribution is averaged over period 1980–1996.

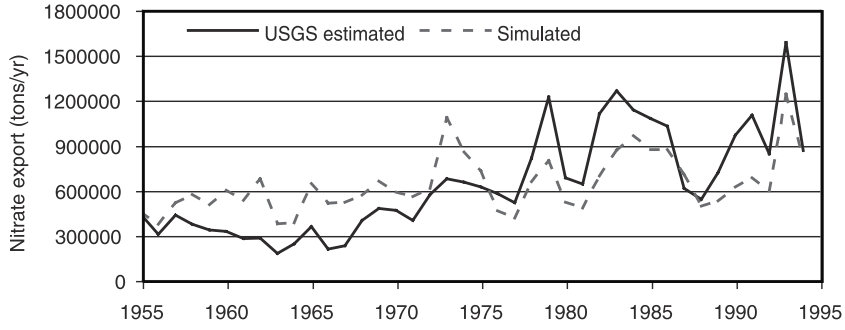

Figure 8. Simulated and USGS estimated annual nitrate export (t yr^{-1}) by Mississippi River at St. Francisville, Louisiana, from 1955 to 1994.

from an average of 328,000 t yr^{-1} for the period 1955–1970 to 925,700 t yr^{-1} for the period 1980–1996 and was accompanied by a substantial increase in interannual variability. As previously stated, this trend has primarily been attributed to the nearly 600% increase in N fertilizer application since the 1950s and to an increase in precipitation and runoff.

[57] Here we compare simulated annual NO_3^- export at St. Francisville from 1955–1994 to this USGS data. Since NO_3^- leaching inputs to the model vary only with runoff over time, the simulated NO_3^- export reflects only the influence of hydrology over time, not an increase in N inputs to the system (i.e., the increase in N-fertilizer application). Therefore, by comparing the simulated and USGS NO_3^- export, we can isolate the role of hydrology in the aforementioned trend and in interannual variability in NO_3^- export.

[58] The simulated annual NO_3^- export of the Mississippi River at St. Francisville, Louisiana, from 1955 to 1994 (Figure 8) captures some of the variability in the USGS record, resulting in significant correlation ($r^2 = 0.54$). An autoregressive model confirmed that autocorrelation among the simulated and observed NO_3^- export time series does not influence the results of the correlation. The index of agreement, a measure of the difference between observed and model-simulated means and variances often used with hydrologic data [*Wilmott et al.*, 1985], also indicated significant correlation ($d = 0.78$). Normal least squares regression of the USGS data indicates an increase of 27,151 t yr^{-1} from 1966 to 1994, significant at the 99% level. In contrast, the simulated NO_3^- export, which captures only the impact of hydrologic change, exhibits a weaker increasing trend of 7112 t yr^{-1}, significant at the 90% level.

[59] We can use the difference between the simulated and observed trends to roughly quantify the role of hydrology in the observed increase in NO_3^- export. The simulated annual increase in export between 1966 and 1994 was 7112 t yr^{-1}, 26% of the annual trend in the USGS data. Additional simulations using the leaching parameters from the sensitivity analysis indicate that the trend could range from 6334 to 8836 t yr^{-1}. This suggests that the observed increase in runoff in the Mississippi Basin is responsible for ~25% of the increase in NO_3^- export between 1966 and 1994, with an error of 7%. The remainder of the observed increase is therefore likely due to an increase in N inputs to the basin, particularly fertilizer application.

[60] The impact of this increase in N inputs to the system partially masks the ability of our hydrology-based model to effectively simulate the interannual variability in export. The simulated export is higher than the USGS estimates from 1955 to 1975, and lower than those from 1976 to 1994, with the exception of 1987. However, the rates employed in the leaching algorithm are based on research conducted during the 1970s; those studies may predict higher NO_3^- leaching than occurred during the earlier period, when drainage practices and N fertilizer application rates likely resulted in

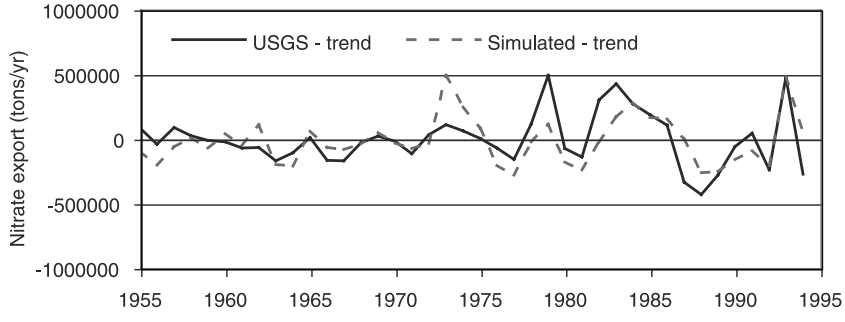

Figure 9. Simulated and USGS estimated "detrended" annual nitrate export anomalies (t yr^{-1}) for Mississippi River at St. Francisville, Louisiana, from 1955 to 1994. Anomalies are difference between annual detrended nitrate export and annual mean detrended nitrate export from 1955 to 1994 (1966–1994 trends are subtracted from both simulated and USGS estimated nitrate exports).

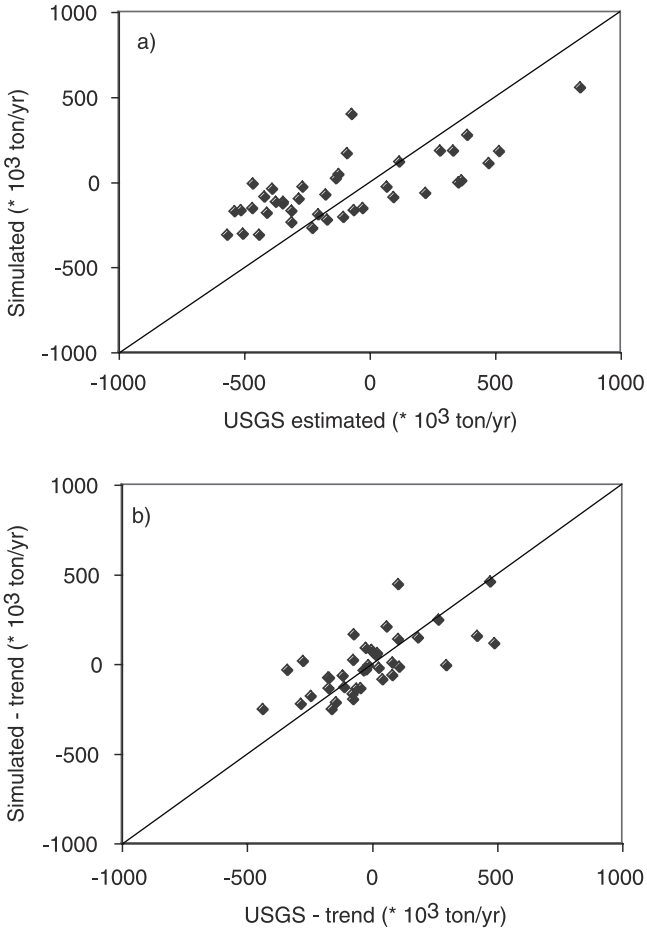

Figure 10. Simulated versus USGS estimated (a) annual nitrate export anomalies (t yr^{-1}) and (b) detrended annual nitrate export anomalies for Mississippi River at St. Francisville, Louisiana, from 1955 to 1994. As in Figure 9, anomalies are difference between annual nitrate export and annual mean nitrate export from 1955 to 1994 for both simulations and observations.

lower leaching rates. The export during early wet years (e.g., 1972) is particularly exaggerated by the model, since in reality, lower N inputs to the land over the earlier period implies less N stored in the soil system available for leaching during a prolonged wet period. As fertilizer and other N inputs increased over the period, soil and groundwater N storage increased. Therefore the Mississippi Basin became increasingly sensitive to hydrologic variability over time, reflected by the large variability in observed annual NO_3^- export since the mid-1970s.

[61] We can demonstrate the strong impact of hydrology on interannual variability in NO_3^- export by subtracting the trends from both simulated and USGS estimated data (Figure 9). With the trends subtracted from both time series, the simulated nitrate export is in closer agreement with the USGS estimates (r^2 = 0.65). The simulated export is still high over the first half of the time period, but there is much closer agreement between the anomalies (Figure 10). The effective simulation of the interannual variability in NO_3^- export illustrates the hydrologic control of NO_3^- leaching and thus illustrates the role of climatic variations in large-scale NO_3^- export.

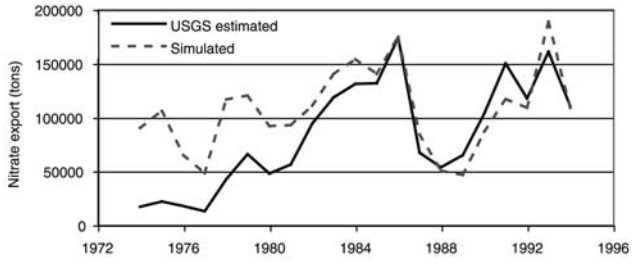

Figure 11. Simulated and USGS estimated annual nitrate export (t yr^{-1}) by Mississippi River at Clinton, Iowa, from 1974 to 1994.

[62] The simulated annual NO_3^- export for the Upper Mississippi Basin at Clinton, Iowa, from 1974 to 1994 is also in close agreement with USGS estimates (r^2 = 0.76; d = 0.81). In both the USGS data and simulations, export increased sharply from 1974 to 1986, dipped during the drier years of 1987–1989, and increased again from 1990 to 1994 (Figure 11). Normal least squares regression indicates an increase of 12936 t yr^{-1} (r^2 = 0.90) from 1974 to 1986 in the USGS data and an increase of 7006 t yr^{-1} (r^2 = 0.60) in the simulated results, both significant at the 99% level. Once again, the agreement between simulations and USGS estimates improves by removing the increasing trends (Figure 12). Removal of 1974–1986 USGS and simulated trends increases the r^2 value to 0.93 and improves agreement between the annual anomalies.

[63] The simulated increase in export from 1974 to 1986 was 7006 t yr^{-1}, 54% of the USGS trend; sensitivity analysis indicates a range of 6075–8225 t yr^{-1}. This suggests that ~55% of the observed increase in export from 1974 to 1986 is due to an increase in runoff in the Upper Mississippi Basin, with an error of 10%. This further emphasizes the pivotal role of hydrologic change and variability in NO_3^- export in the Mississippi Basin.

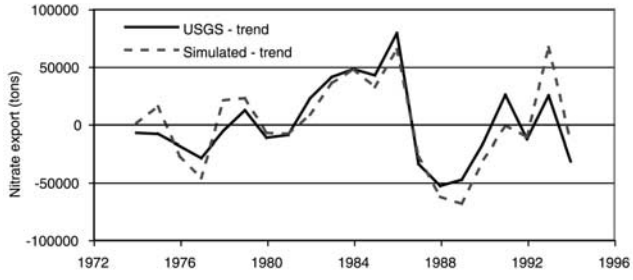

Figure 12. Simulated and USGS estimated detrended annual nitrate export anomalies for Mississippi River at Clinton, Iowa, from 1974 to 1994. Similar to Figure 9, 1974–1986 trends are subtracted from both simulated and USGS estimated nitrate export.

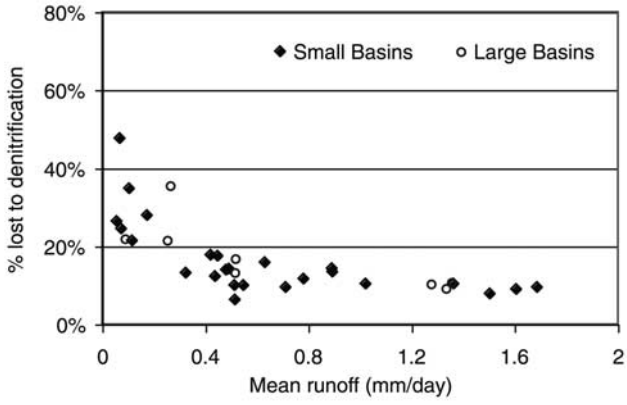

Figure 13. Simulated annual mean nitrate removal versus simulated mean runoff (mm d^{-1}) for eight large and 24 small Mississippi subbasins. Nitrate removal is percent of simulated nitrate mass removed from each basin due to benthic denitrification from 1955 to 1994. Mean runoff is simulated mean annual discharge (1955–1994) from basin divided by basin area.

3.2.3. Denitrification

[64] The simulated annual mean NO_3^- export of the Mississippi River at St. Francisville from 1955 to 1994 is 635,719 t yr^{-1}; without the benthic denitrification function, the simulated export is 769,414 t yr^{-1}. Therefore the model predicts that ~18% of the NO_3^- leached to rivers and streams in the Mississippi Basin is lost to the atmosphere via denitrification in sediments. This estimate of loss due to benthic denitrification is within the 5–20% range predicted by other researchers [*Howarth et al.*, 1996; *Goolsby et al.*, 1999].

[65] There is an inverse relationship between simulated denitrification losses and mean basin runoff (Figure 13). The highest percent of simulated NO_3^- loss occurs in the drier western portion of the Mississippi Basin (e.g., Canadian and Platte Rivers) where shallow, slower rivers permit a large exchange of water with the sediments (Table 5). The lowest percent loss occurs in the main stem of the Mississippi and the more humid eastern portion of the Mississippi Basin (e.g., Tennessee and Allegheny Rivers), since deeper, faster waters limit contact time with the sediments. *Alexander et al.* [2000] noted a similar pattern of

Table 5. Simulated Removal of Nitrate Due to Denitrification, 1955–1994[a]

Large Basins	Location	Basin Area, km^2	Nitrate Loss, %	Error, %
Mississippi	St. Francisville, La.	2,975,468	18	5.0
Upper Mississippi	Clinton, Iowa	226,156	13	7.2
Missouri		1,350,588	22	8.4
Upper Missouri	Omaha, Nebr.	784,655	22	6.7
Lower Missouri	Hermann, Mo.	552,882	22	6.1
Ohio River		518,711	10	1.9
Upper Ohio	Greensboro, Ohio	213,409	10	1.0
Lower Ohio	Metropolis, Ill.	262,124	9	3.6
Middle Mississippi		274,480	17	1.5
Arkansas	Little Rock, Ark.	409,734	36	5.0
Lower Mississippi	St. Francisville, La.	210,570	11	0.0
Wabash	New Harmony, Indiana	72,133	14	5.4
Wisconsin	Muscoda, Wis.	25,539	12	3.1
Missouri	Culbertson, Mont.	223,810	25	2.9
Tennessee	Paducah, Ky.	140,072	9	0.7
Mississippi	Royalton, Minn.	37,467	12	5.2
Minnesota	Jordan, Minn.	52,550	13	14.7
Illinois	Valley City, Ill.	73,411	18	10.0
Canadian	Calvin, Okla.	75,669	48	7.3
Platte	Louisville, Nebr.	260,175	22	5.1
Rock	Joslin, Ill.	23,766	14	9.6
Cedar	Cedar Rapids, Iowa	21,576	14	13.1
Iowa	Wapello, Iowa	32,224	6	11.7
Des Moines	St. Francisville, Mo.	46,144	18	13.0
Yellowstone	Sydney, Mont.	179,341	26	3.0
Kansas	Desoto, Kans.	147,464	28	18.5
Grand	Sumner, Mo.	19,878	10	12.3
Osage	St. Thomas, Mo.	39,088	16	3.1
Arkansas	Tulsa, Okla.	190,618	35	9.0
St. Croix	St. Croix Falls, Wis.	13,920	10	4.7
Chippewa	Durand, Wis.	21,740	10	4.0
Allegheny	New Kensington, Pa.	22,520	10	1.4
Monogahela	Braddock, Pa.	16,596	8	0.5
Muskingham	McConnellsville, Ohio	15,806	13	2.5
Scioto	Higby, Ohio	11,527	10	7.2

[a] Shown are basin name, station location, catchment area, simulated annual mean mass of nitrate removed due to denitrification, and simulated rate of denitrification (per unit of riverbed area). Results represent denitrification losses within each basin (e.g., mass of nitrate removed for Lower Missouri basin does not include mass removed from Upper Missouri basin).

in-stream total N loss across the Mississippi Basin, but reported substantially higher rates of N loss from western portions of the basin. However, that study examined the total N and all forms of N removal, rather than just NO_3^- and denitrification; processes like sedimentation of organic N likely explain the discrepancy.

[66] Validation of simulated denitrification rates, the mass of NO_3^- loss per area of riverbed, is difficult. There are few direct measurements of denitrification in rivers, and most field studies have been limited to a single field season on one river reach [e.g., *Sjodin et al.*, 1997]. Denitrification rates are more often implied indirectly from mass balance models [e.g., *Garcia-Ruiz et al.*, 1998a]. Nevertheless, the simulated mean annual denitrification rates (Table 5) reflect the overall pattern of values reported in the literature [*Billen et al.*, 1991; *Seitzinger*, 1988; *Howarth et al.*, 1996]. Simulated rates for predominately forested basins, like the Tennessee, Allegheny, and Yellowstone, fall close to the reported range (>2 mg m^{-2} h^{-1}) for forested watersheds [*Billen et al.*, 1991]. Rates for intensively cultivated basins, like the Minnesota, Illinois, and Kansas, are much higher and within the reported range (>30 mg m^{-2} h^{-1}) for agricultural watersheds [*Billen et al.*, 1991]. Although the hydrology is a primary limiting factor, denitrification rates tend to be higher in regions of greater crop cover, where NO_3^- loading is greater (Figure 14).

[67] There are extremely few studies of the seasonal range in denitrification rates [*Garcia-Ruiz et al.*, 1998a; *Sjodin et al.*, 1997]. Rates are expected to be highest in the spring and summer, when NO_3^- concentrations are moderate to high and the water temperature is near a peak [*Seitzinger*, 1988; *Pattinson et al.*, 1998]. Simulated mean monthly denitrification rates again follow the expected pattern, with much greater seasonal variability in agricultural watersheds (e.g., Scioto and Wabash Rivers) with high NO_3^- loading (Figure 15). In most locations the simulated denitrification rate reaches a maximum during the summer, later than predicted by field experiments [*Sjodin et al.*, 1997]. Nonetheless, the majority of simulated NO_3^- removal still occurs in the spring, when the denitrification rate may be lower but the actual mass of NO_3^- available for denitrification is much greater.

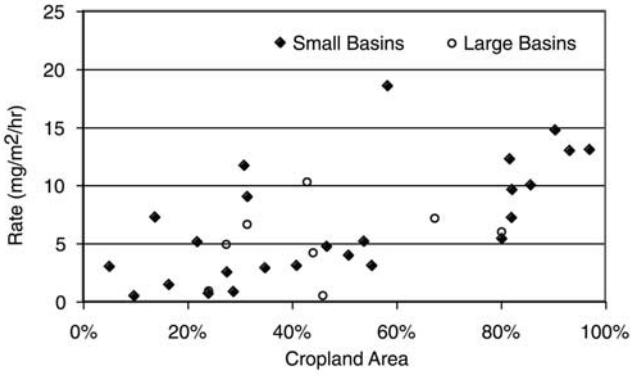

Figure 14. Simulated annual mean denitrification rate (mg m^{-2} hr^{-1}) versus fractional cropland area for eight large and 24 small Mississippi subbasins. Denitrification rates are mass of nitrate removed per unit of riverbed area per hour throughout entire subbasin from 1955 to 1994.

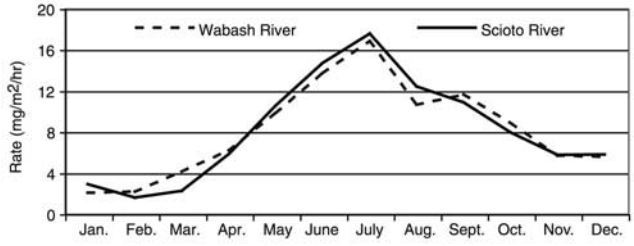

Figure 15. Simulated mean monthly denitrification rates (mg m^{-2} hr^{-1}) for Wabash River Basin in northern Indiana and Scioto River Basin in central Ohio. Denitrification rates are mass of nitrate removed per unit of riverbed area per hour throughout entire watershed from 1955 to 1994.

4. Conclusions

[68] Integrated large-scale studies of the terrestrial and aquatic system are essential for evaluating the impact of potential changes in land use and climate on NO_3^- export. This study is a vital step toward dynamic modeling of NO_3^- export from large river basins like the Mississippi. By combining physical modeling techniques with the existing knowledge of the impact of land cover on NO_3^- export, well demonstrated in previous large-scale modeling studies [e.g., *Caraco and Cole*, 1999], we are able to evaluate the dynamic change in NO_3^- export over time. The modeling system represents much of the spatial and temporal variability in NO_3^- export in the Mississippi River Basin, despite employing a simple method for estimating inputs to the river system.

[69] The ability to simulate the interannual variability in observed NO_3^- export stresses the hydrologic control over interannual changes in NO_3^- leaching and eventual export to the ocean. Although export is fundamentally limited by N inputs to the terrestrial system, hydrologic properties largely determine the proportion of NO_3^- stored in the soil system and the proportion of NO_3^- leached to the aquatic system. Therefore, while the amount of NO_3^- available for leaching in the Mississippi Basin increased dramatically since the mid-1950s, primarily due to a 600% increase in N fertilizer application, the model suggests that an increase in runoff (due to the observed increase in precipitation) was responsible for ~25% of the increase in NO_3^- export to the Gulf of Mexico. The remaining 75% of the increase in NO_3^- export therefore was directly due to the increased input of N to the basin, predominately via fertilizer application.

[70] The modeling system presented here provides the basis for research into the sensitivity of NO_3^- export to climate and land use change in large basins like the Mississippi. The results of this study emphasize that a physically based leaching model, representing spatial variability in soil N processing, a variety of anthropogenic N inputs, and variation in agricultural land management, must be incorporated into IBIS in future studies. Such a

fully integrated physical modeling system could be used to assess the viability of any plan to reduce NO_3^- export by the Mississippi River in the future.

Appendix A: Residence Times and Effective Velocity in HYDRA

[71] The flow of water and nitrate in HYDRA is determined by the time-dependent change in surface, subsurface, and river pools. In this study, the surface and subsurface runoff pools have a constant residency time of 2 hours, since IBIS simulates the delayed passage of water through the soil column. A small fraction (10%) of the subsurface drainage is directed into a groundwater reservoir with a constant residency time of 150 days. This small reservoir guarantees that the simulated rivers will not become completely dry during a drought and has a negligible impact on seasonal or annual discharge.

[72] The river residence time in HYDRA is defined as the distance between the center of the upstream and downstream grid cell divided by the effective velocity of the water. The effective river velocity in HYDRA is proportional to the downstream topographic gradient [*Miller et al.*, 1994; *Coe*, 2000]. However, this relationship underestimates the velocity of large rivers in areas of low topographic relief like the lower Mississippi.

[73] In a model of the water balance of the Amazon Basin, *Costa and Foley* [1997] imposed a minimum effective velocity, which increased with stream order. We developed a similar relationship, where the minimum velocity (u_{min}) is proportional to the ratio of the discharge (Q_c) and a reference discharge (Q_o = 3000 m^3 s^{-1}),

$$u_{min} = u_{om}(Q_c/Q_o)^{0.5},$$

where u_{om} is the absolute minimum velocity (0.3 m s^{-1}).

[74] As the effective velocity is an amalgamation of all river flow and floodplain storage in a grid cell, it is difficult to validate against observed stream velocity. This discharge-based relationship forces the minimum effective velocity to increase downstream, as is typically expected in large rivers.

Appendix B: Nitrate Removal in HYDRA

[75] The denitrification function in HYDRA depends on the area of the riverbed and the mean water temperature in each grid cell. Riverbed area is necessary for calculating the mass of river nitrate removed via denitrification in the sediment. Water temperature is required to simulate the seasonal variation in denitrification rates. The method of dynamically calculating both variables is detailed in sections B1 and B2.

B1. Riverbed Area

[76] In order to define channel morphology and develop a riverbed area relationship, we examined the relationship between average width, depth, cross-sectional area, and discharge for 45 locations on the Mississippi and its major tributaries, taken during USGS sampling cruises [*Moody*, 1993; *Moody and Meade*, 1993, 1995].

[77] In an application of a river flow routing scheme to the Mississippi Basin, *Arora et al.* [1999] assumed the river channel to be trapezoidal. The cross-sectional area (A_c) of a trapezoidal river channel is

$$A_c = wh - h^2/\tan(\theta),$$

where w is the width of the channel, h is the depth of the channel, and θ is the side angle, assumed to be 30° by *Arora et al.* [1999]. The first term is simply the equation for a rectangular channel, and the second term reduces the cross-sectional area to that of a trapezoidal channel. However, since the average river width in the USGS data for the Mississippi and its tributaries is 70 times greater than the average depth, the second term in the trapezoidal equation can be neglected. Therefore a rectangle is a reasonable approximation of river channel shape.

[78] The total riverbed area (A_r) of the rectangular channel of length (l) is

$$A_r = wl + 2hl.$$

[79] Again, since the river width is on average 70 times greater than depth, the second term can be neglected. Therefore the only information necessary for calculating riverbed area is the length of the river reach, already determined from flow direction and grid cell dimensions in HYDRA, and the channel width.

[80] River width can be approximated from a rating curve relationship with discharge ($w = kQ^b$), assuming no significant variation in climate during the time period. *Arora et al.* [1999] estimated that k = 4 and b = 0.56 for the Mississippi Basin, based on data from 13 stations. We determined different constants, using logarithmic regression of average river discharge and channel width from the 45 Mississippi Basin locations referenced above. The regression indicated a highly significant relationship between width and discharge (r^2 = 0.83) with k = 15.75 and b = 0.43. This rating curve is used by HYDRA to determine width and riverbed area, except at very low discharges (<10 m^3 s^{-1}), when the width is approximated by the discharge. Width and riverbed area are determined at each time step only for calculating the rate of denitrification and do not influence the downstream transport of water and nitrate.

B2. Water Temperature

[81] River or stream temperature has been simulated in the past with physical models, based on heat advection and transport or the surface energy balance [*Mohseni and Stefan*, 1999]. However, since the surface water temperature is primarily controlled by air temperature, and the water column in rivers is typically isothermal, the average stream temperature can be closely approximated from the ambient air temperature [*Mohseni et al.*, 1998]. In this study, we determined the monthly water temperature (T_s) from the monthly air temperature (T_a) using a simple empirical relationship developed by *Mohseni et al.* [1998] in a study of 584 river stations throughout the United States, nearly half of which lie within the Mississippi Basin:

$$T_s = \mu + (\alpha - \mu)/(1 + \exp(\gamma(\beta - T_a))),$$

where α = 26.2°C (maximum observed T_s), β = 13.3°C (T_a at inflection point of curve), γ = 0.18°C^{-1} (steepest slope of function), and μ = 0.8°C^{-1} (minimum observed T_s). Average parameter values are chosen for simplicity.

[82] Unlike simple linear air-water temperature equations, this curvilinear relationship better represents low water temperatures and the moderating effect of evaporative cooling at high air temperatures [*Mohseni et al.*, 1998]. *Mohseni et al.* [1998] reported that the relationship accurately simulated weekly stream temperatures at 89% of the 584 stations studied, with the majority of the errors occurring near reservoirs or high wastewater and groundwater inputs. In a supplemental test, the equation accurately predicted the observed Mississippi River temperatures (available from U.S. Geological Survey, water-quality and streamflow data, at http://wwwrvares.er.usgs.gov/wqn96cd/html/wqn/wq/). over a 3-year period at both Alton, Illinois (r^2 = 0.93), and Arkansas City, Arkansas (r^2 = 0.90).

[83] **Acknowledgments.** We would like to thank Donald Goolsby for providing the annual nitrate flux data and numerous USGS reports on the Mississippi River and Paul Whitehead for his insight on simulating denitrification rates in rivers. We would also like to thank Mary Sternitzky for technical assistance in preparing the manuscript. Two anonymous reviewers offered many helpful comments and suggestions that have significantly improved the quality of the manuscript. This research was supported by the NASA Office of Earth Science, a NASA Earth Systems Science Graduate fellowship, and the Climate, People and Environment Program of the University of Wisconsin.

References

Alexander, R. B., and R. A. Smith, County-level estimates of nitrogen and phosphorus fertilizer use in the United States, 1945 to 1985, *U.S. Geol. Surv. Open File Rep., 90-130*, 1990.

Alexander, R. B., R. A. Smith, and G. E. Schwarz, Effect of stream channel size on the delivery of nitrogen to the Gulf of Mexico, *Nature*, *403*, 758–761, 2000.

Arora, V. K., F. H. S. Chiew, and R. B. Grayson, A river flow routing scheme for general circulation models, *J. Geophys. Res.*, *104*(D12), 14,347–14,357, 1999.

Baldwin, C. K., and U. Lall, Seasonality of streamflow: The upper Mississippi River, *Water Resour. Res.*, *35*(4), 1143–1154, 1999.

Battaglin, W. A., C. Kendall, C. C. Y. Chang, S. R. Silva, and D. H. Campbell, Chemical and isotopic evidence of nitrogen transformation in the Mississippi River, 1997–98, *Hydrol. Processes*, *15*(7), 1285–1300, 2001.

Billen, G., C. Lancelot, and M. Meybeck, N, P, Si retention along the aquatic continuum from land to ocean, in *Ocean Margin Processes in Global Change*, edited by R. F. C. Mantoura, J. M. Martin, and R. Wollast, pp. 19–44, John Wiley, New York, 1991.

Burkart, M. R., and D. E. James, Agricultural-nitrogen contributions to hypoxia in the Gulf of Mexico, *J. Environ. Qual.*, *28*, 850–859, 1999.

Caraco, N. F., and J. J. Cole, Human impact on nitrate export: An analysis using major world rivers, *Ambio*, *28*(2), 167–170, 1999.

Carey, A. E., W. B. Lyons, J. C. Bonzongo, and J. C. Lehrter, Nitrogen budget in the Upper Mississippi River watershed, *Environ. Eng. Geosci.*, *7*(3), 251–265, 2001.

Coe, M. T., A linked global model of terrestrial hydrologic processes: Simulation of modern rivers, lakes, and wetlands, *J. Geophys. Res.*, *103*(D8), 8885–8899, 1998.

Coe, M. T., Modeling terrestrial hydrological systems at the continental scale: Testing the accuracy of an atmospheric GCM, *J. Clim.*, *13*(4), 686–704, 2000.

Coe, M. T., and J. A. Foley, Human and natural impacts on the water resources of the Lake Chad Basin, *J. Geophys. Res.*, *106*(D4), 3349–3356, 2001.

Costa, M. H., and J. A. Foley, Water balance of the Amazon Basin: Dependence on vegetation cover and canopy conductance, *J. Geophys. Res.*, *102*(D20), 23,973–23,989, 1997.

Creed, I. F., and L. E. Band, Export of nitrogen from catchments within a temperate forest: Evidence for a unifying mechanism regulated by variable source area dynamics, *Water Resour. Res.*, *34*(11), 3105–3120, 1998.

Diaz, R. J., and R. Rosenberg, Marine benthic hypoxia: A review of its ecological effects and the behavioral responses of benthic macrofauna, *Oceanogr. Mar. Biol. Annu. Rev.*, *33*, 245–303, 1995.

Dodds, W. K., J. M. Blair, G. M. Henebry, J. K. Koelliker, and R. Ramundo, Nitrogen transport from tallgrass prairie watersheds, *J. Environ. Qual.*, *25*, 973–981, 1996.

Ferrier, R. C., et al., Modeling impacts of land-use change and climate-change on nitrate-nitrogen in the River Don, North-East Scotland, *Water Res.*, *29*(8), 1950–1956, 1995.

Foley, J. A., et al., An integrated biosphere model of land surface processes, terrestrial carbon balance, and vegetation dynamics, *Global Biogeochem. Cycles*, *10*(4), 603–628, 1996.

Galloway, J. N., W. H. Schlesinger, and H. Levy II, et al., Nitrogen fixation: Anthropogenic enhancement-environmental response, *Global Biogeochem. Cycles*, *9*(2), 235–252, 1995.

Garcia-Ruiz, R., S. N. Pattinson, and B. A. Whitton, Denitrification and nitrous oxide production in sediments of the Wiske, a lowland eutrophic river, *Sci. Total Environ.*, *210/11*, 307–320, 1998a.

Garcia-Ruiz, R., S. N. Pattinson, and B. A. Whitton, Denitrification in river sediments: relationship between process rate and properties of water and sediment, *Freshwater Biol.*, *39*(3), 467–476, 1998b.

Geng, S., F. W. T. Penning de Vries, and I. Supit, A simple method for generating daily rainfall data, *Agric. For. Meteorol.*, *36*, 363–376, 1985.

Goolsby, D. A., et al., Flux and sources of nutrients in the Mississippi-Atchafalaya River basin: Topic 3 report for the integrated assessment on hypoxia in the Gulf of Mexico, *NOAA Coastal Ocean Prog. Decision Anal. Ser. 17*, 130 pp., NOAA Coastal Ocean Off., Silver Spring, Md., 1999.

Goolsby, D. A., W. A. Battaglin, B. T. Aulenbach, and R. P. Hooper, Nitrogen flux and sources in the Mississippi River Basin, *Sci. Total Environ.*, *248*, 75–86, 2000.

Howarth, R. W., G. Billen, D. Swaney, et al., Regional nitrogen budgets and riverine N and P fluxes for the drainages to the North Atlantic Ocean: Natural and human influences, *Biogeochemistry*, *35*, 75–139, 1996.

Johnes, P. J., Evaluation and management of the impact of land use change on the nitrogen and phosphorus load delivered to surface waters: The export coefficient modeling approach, *J. Hydrol.*, *183*(3–4), 323–349, 1996.

Kucharik, C. J., J. A. Foley, C. Delire, et al., Testing the performance of a dynamic global ecosystem model: Water balance, carbon balance, and vegetation structure, *Global Biogeochem. Cycles*, *14*(3), 795–825, 2000.

Lawrence, G. B., D. A. Goolsby, W. A. Battaglin, and G. J. Stensland, Atmospheric nitrogen in the Mississippi River Basin: Emissions, deposition and transport, *Sci. Total Environ.*, *248*, 87–99, 2000.

Lenters, J. D., M. T. Coe, and J. A. Foley, Surface water balance of the continental United States, 1963–1995: Regional evaluation of a terrestrial biosphere model and the NCEP/NCAR reanalysis, *J. Geophys. Res.*, *105*(D17), 22,393–22,425, 2000.

Loehr, R. C., Characteristics and comparative magnitude of non-point sources, *J. Water Pollut. Control Fed.*, *46*, 1849–1872, 1974.

Loveland, T. R., and A. S. Belward, The IGBP-DIS global 1 km land cover data set, DISCover, *Int. J. Remote Sens.*, *18*, 3289–3295, 1997.

Lucey, K. J., and D. A. Goolsby, Effects of climate variation over 11 years on nitrate-nitrogen concentrations in the Raccoon River, Iowa, *J. Environ. Qual.*, *22*, 38–46, 1993.

Meybeck, M., Carbon, nitrogen and phosphorous transport by world rivers, *Am. J. Sci.*, *282*, 401–450, 1982.

Miller, D. A., and R. A. White, A conterminous United States multi-layer soil characteristics data set for regional climate and hydrology modeling, *Earth Interact.*, *2*, Available online at http://EarthInteractions.org, 1998.

Miller, J. R., G. L. Russell, and G. Caliri, Continental-scale river flow in climate models, *J. Clim.*, *7*, 914–928, 1994.

Mohseni, O., and H. G. Stefan, Stream temperature air temperature relationship: A physical interpretation, *J. Hydrol.*, *218*(3–4), 128–141, 1999.

Mohseni, O., H. G. Stefan, and T. R. Erickson, A nonlinear regression model for weekly stream temperatures, *Water Resour. Res.*, *34*(10), 2685–2692, 1998.

Moody, J. A., Evaluation of the Lagrangian scheme for sampling the Mississippi River during 1987–90, *U.S. Geol. Surv. Open File Rep., 93-4042*, 31 pp., 1993.

Moody, J. A., and R. H. Meade, Hydrologic and sedimentologic data collected during four cruises at high water on the Mississippi River and some of it tributaries, *U.S. Geol. Surv. Open File Rep., 92-651*, 227 pp., 1993.

Moody, J. A., and R. H. Meade, Hydrologic and sedimentologic data

collected during three cruises on the Mississippi River and some of it tributaries from Minneapolis, Minnesota to New Orleans, Louisiana, July 1991, May 1992, *U.S. Geol. Surv. Open File Rep., 94-474*, 159 pp., 1995.

Naqvi, S. W. A., D. A. Jayakumar, P. V. Narvekar, et al., Increased marine production of N_2O due to intensifying anoxia on the Indian continental shelf, *Nature*, *408*, 346–349, 2000.

New, M., M. Hulme, and P. D. Jones, Representing twentieth-century space-time climate variability, II, Development of a 1901–1996 monthly terrestrial climate fields, *J. Clim.*, *13*, 2217–2238, 2000.

Pattinson, S. N., R. Garcia-Ruiz, and B. A. Whitton, Spatial and seasonal variation in denitrification in the Swale-Ouse system, a river continuum, *Sci. Total Environ.*, *210/11*, 289–305, 1998.

Peterson, B. J., W. M. Wollheim, and P. J. Mulholland, et al., Control of nitrogen export from watersheds by headwater streams, *Science*, *292*, 86–89, 2001.

Rabalais, N. N., R. E. Turner, D. Justic, et al., Nutrient changes in the Mississippi River and system responses on the adjacent continental shelf, *Estuaries*, *19*(28), 366–407, 1996.

Ramankutty, N., and J. A. Foley, Characterizing patterns of global land use: An analysis of global croplands data, *Global Biogeochem. Cycles*, *12*(4), 667–685, 1998.

Ramankutty, N., and J. A. Foley, Estimating historical changes in land cover: North American croplands from 1850 to 1992, *Global Ecol. Biogeogr.*, *8*(5), 381–396, 1999.

Randall, G. W., D. R. Huggins, M. P. Russelle, et al., Nitrate losses through subsurface tile drainage in Conservation Reserve Program, alfalfa, and row crop systems, *J. Environ. Qual.*, *26*, 1240–1247, 1997.

Reckhow, K. H., M. N. Beaulac, and J. J. Simpson, Modeling phosphorus loading and Lake response under uncertainty: A manual and compilation of export coefficients, *EPA-440/5-80-011*, 214 pp., U.S. Environ. Prot. Agency, Washington, D. C., 1980.

Richardson, C. W., Stochastic simulation of daily precipitation, temperature, and solar radiation, *Water Resour. Res.*, *17*(1), 182–190, 1981.

Seitzinger, S. P., Denitrification in freshwater and coastal marine ecosystems: Ecological and geochemical significance, *Limnol. Oceanogr.*, *33*(4), 702–724, 1988.

Seitzinger, S. P., and C. Kroeze, Global distribution of nitrous oxide production and N inputs in freshwater and coastal marine ecosystems, *Global Biogeochem. Cycles*, *12*(1), 93–113, 1998.

Showstack, R., Nutrient overenrichment implicated in multiple problems in U.S. waterways, *Eos Trans. AGU*, *81*(43), 497, 2000.

Sjodin, A. L., W. M. Lewis, and J. F. Saunders, Denitrification as a component of the nitrogen budget for a large plains river, *Biogeochemistry*, *39*, 327–342, 1997.

Toms, I. P., M. J. Mindenhall, and M. M. I. Harman, Factors affecting the removal of nitrate by sediments from rivers, lagoons and lakes, *Tech. Rep. TR14*, Water Res. Cent., Wiltshire, England, 1975.

Turner, R. E., and N. N. Rabalais, Changes in Mississippi River water-quality this century, *Bioscience*, *41*(3), 140–147, 1991.

Turner, R. E., and N. N. Rabalais, Coastal eutrophication near the Mississippi River delta, *Nature*, *368*, 619–621, 1994.

U.S. Department of Agriculture, Major world crop areas and climatic profiles, *USDA Agric. Handb. 664*, Washington, D. C., 1994.

Vorosmarty, C. J., B. M. Fekete, and B. A. Tucker, *Global River Discharge Database (RivDIS v1.0),* vol. 0, *Introduction, Overview, and Technical Notes*, Int. Hydrol. Prog., U.N. Educ., Sci., and Cult. Org., Paris, 1996.

Whitehead, P. G., R. J. Williams, and D. R. Lewis, Quality simulation along river systems (QUASAR): Model theory and development, *Sci. Total Environ.*, *194*, 447–456, 1997.

Wilmott, C. J., S. G. Ackleson, R. E. Davis, et al., Statistics for the evaluation and comparison of models, *J. Geophys. Res.*, *90*(C5), 8995–9005, 1985.

Wu, J. J., and B. A. Babcock, Metamodeling potential nitrate water pollution in the central United States, *J. Environ. Qual.*, *28*, 1916–1928, 1999.

Zucker, L. A., and L. C. Brown (Eds.), Agricultural drainage: Water quality impacts and subsurface drainage studies in the Midwest, *Bull. 871*, 40 pp., Ohio State Univ. Ext., Columbus, Ohio, 1998.

M. T. Coe, S. D. Donner, J. A. Foley, J. D. Lenters, and T. E. Twine, Center for Sustainability and the Global Environment (SAGE), Institute for Environmental Studies, University of Wisconsin-Madison, 1255 West Dayton Street, Madison, WI 53706, USA. (sdonner@wisc.edu)